Multipartite entanglement at dynamical quantum phase transitions with nonuniformly spaced criticalities

Stav Haldar,[1,2] Saptarshi Roy,[1] Titas Chanda,[3,*] Aditi Sen(De),[1] and Ujjwal Sen[1]
[1]*Harish-Chandra Research Institute, HBNI, Chhatnag Road, Jhunsi, Allahabad 211 019, India*
[2]*Hearne Institute for Theoretical Physics and Department of Physics and Astronomy, Louisiana State University, Baton Rouge, Louisiana 70803, USA*
[3]*Instytut Fizyki Teoretycznej, Uniwersytet Jagielloński, Łojasiewicza 11, 30-348 Kraków, Poland*

(Received 28 March 2019; revised manuscript received 10 May 2020; accepted 11 May 2020; published 12 June 2020)

We report a dynamical quantum phase transition portrait in the alternating field transverse XY spin chain with Dzyaloshinskii-Moriya interaction by investigating singularities in the Loschmidt echo and the corresponding rate function after a sudden quench of system parameters. Unlike the Ising model, the analysis of the Loschmidt echo yields nonuniformly spaced transition times in this model. Comparative study between the equilibrium and the dynamical quantum phase transitions in this case reveals that there are quenches where one occurs without the other and reveals the regimes where they coexist. However, such transitions happen only when quenching is performed across at least a single gapless or critical line. Contrary to equilibrium phase transitions, bipartite entanglement measures do not turn out to be useful for the detection, while multipartite entanglement emerges as a good identifier of this transition when the quench is done from a disordered phase of this model.

DOI: 10.1103/PhysRevB.101.224304

I. INTRODUCTION

Quantum many-body systems can undergo phase transitions due to a variation in the system parameters at temperatures very close to absolute zero—entirely driven by quantum fluctuations [1]. Typically, quantum critical points are identified by a vanishing energy gap and divergence in characteristic correlation lengths, thereby leading to singularities in physical quantities [2,3]. In recent years, bipartite as well as multipartite entanglement [4] have been proposed to be detectors of quantum phase transitions [5–7]. Traditional or classical phase transitions (CPTs) are qualitatively different from quantum ones since CPTs are induced by thermal fluctuations.

Quantum systems, in addition to equilibrium transitions, can also display nonanalyticities during dynamics, a phenomenon coined as dynamical quantum phase transition (DQPT) [8–13] and that is traditionally detected by singularities of a certain distance function between the initial and the final time-evolved states, known as the Loschmidt echo [14].

Extensive DQPT studies have been performed in one-dimensional quantum spin models like XY [8,9,15–21] and XXZ [22] models under different types of quenches [23], and several counterintuitive results have been reported regarding the relation between the equilibrium quantum phase transition (EQPT) and the DQPT [19,22]. More importantly, DQPTs have been experimentally observed in trapped ions [24] and in fermionic systems in a hexagonal lattice undergoing a topological DQPT [25] (see also Ref. [26]). It is as yet not clear whether entanglement can be useful for detecting DQPTs. Some initial results in this direction indicate that a vanishing Schmidt gap can be related to the zeros of the Loschmidt echo [27] at critical times of the DQPT in the transverse Ising spin chain. Apart from the fundamental importance of such studies, with entanglement, it may have important implications in the design of quantum technologies like one-way and topological quantum computers and quantum simulators [28–33].

In this paper, we examine the DQPT for a uniform and alternating transverse field XY spin chain (ATXY) in the presence of an additional antisymmetric interaction, the Dzyaloshinskii-Moriya (DM) interaction [34–67] via both the traditional and the information theoretic approach. For the DATXY model, we analytically compute the Loschmidt echo and its corresponding critical times which turn out to be nonuniformly spaced for most general quenches of the system parameters, viz., the uniform field, the alternating field, and the DM interaction strength. The quenches are performed both within and across the equilibrium phase boundaries. The DATXY model reduces to various well-known models like Ising, UXY, XX, etc., in different limits of the system parameters, and reproduces the critical times of the DQPT for the same [8]. Such a general model is chosen because the reduced models, in the case of DQPTs, have been shown not to capture the relevant physics in its full generality. For example, the Ising model predicts an equivalence between the EQPT and the DQPT [8], although later this was shown not to be the case even for the UXY model [19] (see also Ref. [22]). The results for the DATXY model also confirms this inequivalence. Moreover, our results provide a necessary condition on the quenches that leads to a DQPT, namely, *a quench corresponding to a DQPT must cross at least one equilibrium critical line.*

On the other hand, systematic studies reveal that unlike in the EQPT, bipartite entanglement fails as a detector for the DQPT. However, we find that if the initial state belongs

*titas.chanda@uj.edu.pl

to a disordered phase, genuine multipartite entanglement *can* identify a DQPT. Specifically, we observe that the time-averaged standard deviation of a geometric measure of multipartite entanglement [68] (see also Refs. [69–72]) has *much* higher values when the final quench point falls in a region that corresponds to a DQPT than when it falls in regions without it. The regions show a large overlap with those detected through singularities in the Loschmidt echo. Our observation also indicates that a low value of multipartite entanglement in the initial state, which indeed is a feature of ground states in the disordered phase, can be a plausible explanation for this asymmetric identification of DQPT with multiparty entanglement.

The paper is organized as follows. The model Hamiltonian, its diagonalization, and its ground-state phases are discussed in Sec. II. In Sec. III, the DQPT exhibited by the model is analyzed via the Loschmidt echo, while the same is reanalyzed by the tools of quantum information theory, namely by employing bipartite and genuine multipartite entanglement in Sec. IV. We finally conclude in Sec. V.

II. TRANSVERSE XY MODEL WITH ALTERNATING FIELD AND ANTISYMMETRIC INTERACTION

We consider a paradigmatic family of interacting quantum spin-1/2 systems on a one-dimensional (1D) lattice with nearest-neighbor anisotropic XY interaction as well as asymmetric DM interaction in the presence of uniform and alternating external transverse magnetic fields described by the following Hamiltonian [34]:

$$\hat{H} = \frac{1}{2}\sum_{j=1}^{N}\Bigg[J\left(\frac{1+\gamma}{2}\hat{\sigma}_j^x\hat{\sigma}_{j+1}^x + \frac{1-\gamma}{2}\hat{\sigma}_j^y\hat{\sigma}_{j+1}^y\right) + \frac{D}{2}\left(\hat{\sigma}_j^x\hat{\sigma}_{j+1}^y - \hat{\sigma}_j^y\hat{\sigma}_{j+1}^x\right) + [h_1 + (-1)^j h_2]\hat{\sigma}_j^z\Bigg], \quad (1)$$

with a periodic boundary condition, i.e., $\hat{\sigma}_{N+1} = \hat{\sigma}_1$. Here, $\hat{\sigma}^\alpha$ ($\alpha = x, y, z$) are the Pauli matrices; J and D represent the strengths of the nearest-neighbor exchange interaction and the DM interaction, respectively; γ ($\neq 0$) is the anisotropy parameter for the xx and yy interactions; h_1 and h_2 are the uniform and alternating transverse magnetic fields, respectively; and N denotes the total number of lattice sites. The Hamiltonian, referred to as the DATXY model, can be mapped to a spinless 1D Fermi system with two sublattices (for even and odd sites) via the Jordan-Wigner transformation [34,73]. Further, performing Fourier transformation, the Hamiltonian can be block-diagonalized in the momentum space, as $\hat{H} = \sum_{p=1}^{N/4}\hat{H}_p$, with

$$\begin{aligned}\hat{H}_p = J[&(\cos\phi_p + d\sin\phi_p)(a_p^\dagger b_p + b_p^\dagger a_p)\\ &+ (\cos\phi_p - d\sin\phi_p)(a_{-p}^\dagger b_{-p} + b_{-p}^\dagger a_{-p})\\ &- i\gamma\sin\phi_p(a_p^\dagger b_{-p} + a_p b_{-p} - a_{-p}^\dagger b_p^\dagger - a_{-p}b_p)\\ &+ (\lambda_1+\lambda_2)(b_p^\dagger b_p + b_{-p}^\dagger b_{-p})\\ &+ (\lambda_1-\lambda_2)(b_p^\dagger b_p + b_{-p}^\dagger b_{-p}) - 2\lambda_1], \end{aligned} \quad (2)$$

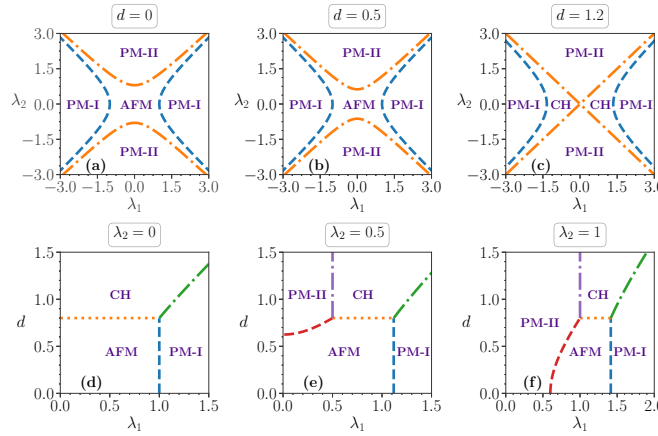

FIG. 1. Phase diagrams of the DATXY model in different parameter spaces. Here, we choose $\gamma = 0.8$. Unless otherwise stated, we use $\gamma = 0.8$ throughout the paper for demonstration purposes. All quantities plotted are dimensionless.

where $\lambda_i = h_i/J$, with $i = 1$ and 2; $d = D/J$ are the dimensionless system parameters; $\phi_p = 2\pi p/N$; and $\hat{a}_p$ ($\hat{b}_p$) corresponds to the fermionic operators for odd (even) sublattices. Therefore, diagonalization of $\hat{H}$, required to study its characteristics, reduces in diagonalizing $\hat{H}_p$ for different momentum sectors, which can be done by proper choice of the basis [34,73]. In equilibrium, this model can exhibit two paramagnetic phases (PM-I and PM-II), an antiferromagnetic phase (AFM), and a *gapless* chiral (CH) phase (see Ref. [34]).

It is noteworthy to mention that several well-known quantum spin models in different parameter regimes can be obtained from the DATXY model, such as

(i) the transverse field Ising (TFI) model for $\gamma = 1$ and $\lambda_2 = d = 0$,

(ii) the quantum XY model with a uniform magnetic field (UXY) for $\lambda_2 = d = 0$,

(iii) the quantum XY model with uniform and alternating magnetic fields (ATXY) [3,73–76] for $d = 0$, and

(iv) the quantum XY model with a uniform magnetic field in the presence of DM interaction (DUXY) for $\lambda_2 = 0$.

We choose the DATXY model for demonstration, as this model possesses a very rich phase diagram at zero temperature (see Fig. 1). Moreover, we notice that by fixing different parameters suitably, it can be reduced to any of the above four models. The equilibrium quantum phase transitions between these different phases occur across the following surfaces [34]:

(i) for $0 \leqslant d < \gamma$,
  (a) $\lambda_1^2 = 1 + \lambda_2^2$ (PM-I $\leftrightarrow$ AFM),
  (b) $\lambda_2^2 = \lambda_1^2 + \gamma^2 - d^2$ (PM-II $\leftrightarrow$ AFM),

(ii) for $d > \gamma$,
  (a) $\lambda_1^2 = 1 + \lambda_2^2 + d^2 - \gamma^2$ (PM-I $\leftrightarrow$ CH),
  (a) $\lambda_1 = \pm\lambda_2$ (PM-II $\leftrightarrow$ CH).

Note that, in the thermodynamic limit, the AFM phase of the spin Hamiltonian given in Eq. (1) has twofold degeneracy, whereas in the fermionic version of the model, the ground state in that phase is unique. The AFM phase appears for $d < \gamma$, whereas for $d > \gamma$, we get the CH phase. The gapless CH phase, in addition to having a continuous spectra, has a threefold degenerate ground state.

III. DYNAMICAL QUANTUM PHASE TRANSITIONS IN DATXY MODEL

Let us now move to investigate DQPTs in the DATXY model. At $t = 0$, we prepare the system in a ground state of a Hamiltonian, $\hat{H}^{(0)} = \hat{H}(g_0)$, with initial parameter values, $g_0 \equiv \{\lambda_1(t=0), \lambda_2(t=0), d(t=0)\}$, and then at $t > 0$, we suddenly quench the system parameters to new values, $g_1 \equiv \{\lambda_1(t>0), \lambda_2(t>0), d(t>0)\}$, such that the new Hamiltonian becomes $\hat{H}^{(1)} = \hat{H}(g_1)$, according to which the system evolves with time. Note that, unless otherwise stated, we will not change the anisotropy parameter γ in the quenching process.

Loschmidt amplitude and Loschmidt echo

Analogous to the role of canonical partition function in temperature-driven phase transitions, the Loschmidt amplitude is shown to play an important role in DQPTs [8,9] and is defined as the overlap of the time-evolved state of a system with its initial state. If the initial state, $|\Psi^0\rangle$, is prepared as the ground state of the initial Hamiltonian, $\hat{H}^{(0)}$, and the Hamiltonian after the quench is $\hat{H}^{(1)}$, then the Loschmidt amplitude is defined as

$$G(t) = \langle\Psi^0| e^{-i\hat{H}^{(1)}t/\hbar} |\Psi^0\rangle . \tag{3}$$

For quenching in the parameter space of the DATXY model, using Eq. (2), the above expression can be decomposed as

$$G(t) = \prod_{p=1}^{N/4} \langle\Psi_p^0| e^{-i\hat{H}_p^{(1)}t/\hbar} |\Psi_p^0\rangle = \prod_{p=1}^{N/4} G_p(t), \tag{4}$$

where $|\Psi_p^0\rangle$ is the eigenstate of $\hat{H}_p^{(0)}$ corresponding to the lowest eigenvalue, and in the last expression, we have defined the Loschmidt amplitude per momentum mode as $G_p(t) = \langle\Psi_p^0| e^{-i\hat{H}_p^{(1)}t/\hbar} |\Psi_p^0\rangle$. The Loschmidt echo $L(t)$ is then described by the probability associated with this amplitude, i.e., $L(t) = |G(t)|^2$. The rate function associated with $L(t)$, which is analogous to the free energy (per lattice site) in thermal phase transitions, can be defined as

$$\mathcal{F}(t) = -\lim_{N\to\infty} \frac{1}{N} \log L(t) = -\lim_{N\to\infty} \frac{2}{N} \sum_{p=1}^{N/4} \log |G_p(t)|. \tag{5}$$

Similar to the thermal phase transition, where transition is dictated by the nonanalytic behavior of the associated free energy with respect to the temperature, the DQPT can be detected by the nonanalyticity of the rate function as a function of time at some critical time t^*.

To deduce the analytical expressions of the Loschmidt amplitude and the rate function for a general quench from $g_0 \equiv \{\lambda_1(t=0), \lambda_2(t=0), d(t=0)\}$ to $g_1 \equiv \{\lambda_1(t>0), \lambda_2(t>0), d(t>0)\}$, we introduce the fermionic vector operator $\hat{A}_p = [\hat{a}_p, \hat{b}_p]$. We then perform a Bogoliubov transformation of the following form:

$$\begin{bmatrix} \hat{A}_p \\ \hat{A}^\dagger_{-p} \end{bmatrix} = M_p \begin{bmatrix} \hat{\Gamma}_p \\ \hat{\Gamma}^\dagger_{-p} \end{bmatrix} = \begin{bmatrix} U_p & -iV_p \\ -iV_p^* & U_p^* \end{bmatrix} \begin{bmatrix} \hat{\Gamma}_p \\ \hat{\Gamma}^\dagger_{-p} \end{bmatrix}, \tag{6}$$

with $\hat{\Gamma}_p = [\hat{\eta}_p^a, \hat{\eta}_p^b]$, such that $\hat{H}_p$ is diagonal in the Bogoluibov basis, $\{\hat{\eta}_p^{a\dagger}, \hat{\eta}_p^{b\dagger}, \hat{\eta}_{-p}^a, \hat{\eta}_{-p}^b\}$. U_p and V_p are Bogoliubov coefficients (matrices) and are functions of $g \equiv \{\lambda_1, \lambda_2, d\}$.

In order to calculate $\langle\Psi^0| e^{-iH^{(1)}t/\hbar} |\Psi^0\rangle$, we express the operators $\{\hat{\Gamma}_p(g_0)\}$ that diagonalize the initial Hamiltonian $\hat{H}^{(0)}$ in terms of $\{\hat{\Gamma}_p(g_1)\}$ which diagonalize the final Hamiltonian $\hat{H}^{(1)}$ using Eq. (6) as

$$\begin{bmatrix} \hat{\Gamma}_p(g_0) \\ \hat{\Gamma}^\dagger_{-p}(g_0) \end{bmatrix} = \begin{bmatrix} \mathcal{U}_p(g_0,g_1) & -i\mathcal{V}_p(g_0,g_1) \\ -i\mathcal{V}_p^*(g_0,g_1) & \mathcal{U}_p^*(g_0,g_1) \end{bmatrix} \begin{bmatrix} \hat{\Gamma}_p(g_1) \\ \hat{\Gamma}^\dagger_{-p}(g_1) \end{bmatrix}, \tag{7}$$

with

$$\begin{aligned} \mathcal{U}_p(g_0,g_1) &= U_p^\dagger(g_0)U_p(g_1) + V_p^T(g_0)V_p^*(g_1), \\ \mathcal{V}_p(g_0,g_1) &= U_p^\dagger(g_0)V_p(g_1) - V_p^T(g_0)U_p^*(g_1). \end{aligned} \tag{8}$$

We can now write the initial state $|\Psi^0\rangle$ as a boundary state composed of zero-momentum modes of $\hat{H}^{(1)}$, given by

$$|\Psi^0\rangle = \mathcal{N}^{-1} \exp\left[i \sum_{p=1}^{N/4} \hat{\Gamma}_p^{\dagger T} \left(\mathcal{U}_p^{-1}\mathcal{V}_p\right) \hat{\Gamma}^\dagger_{-p} \right] |0\rangle, \tag{9}$$

where $|0\rangle$ is the ground state of $\hat{H}^{(1)}$, $\mathcal{N}$ is the normalization constant, and T denotes the transpose of the corresponding operators. By using eigenvalues $\hbar\omega_p^k$ ($k = 1, 2, 3, 4$) of $\hat{H}_p^{(1)} = \hat{A}_p^\dagger \tilde{H}_p^{(1)} \hat{A}_p$, where $\hat{A}_p$ is the column vector, $(\hat{a}_p, \hat{b}_p, \hat{a}^\dagger_{-p}, \hat{b}^\dagger_{-p})$, and

$$\tilde{H}_p^{(1)} = J \begin{bmatrix} (\lambda_1-\lambda_2) & (\cos\phi_p + d\sin\phi_p) & 0 & -i\gamma\sin\phi_p \\ (\cos\phi_p + d\sin\phi_p) & (\lambda_1+\lambda_2) & -i\gamma\sin\phi_p & 0 \\ 0 & i\gamma\sin\phi_p & -(\lambda_1-\lambda_2) & -(\cos\phi_p - d\sin\phi_p) \\ i\gamma\sin\phi_p & 0 & -(\cos\phi_p - d\sin\phi_p) & -(\lambda_1+\lambda_2) \end{bmatrix}, \tag{10}$$

with $\phi_p \in [-\pi/2, \pi/2]$, we obtain

$$\begin{aligned} G_p(t) = {} & e^{i\frac{Jt}{\hbar}(\omega_p^3+\omega_p^4)} \\ & \times \frac{1 + e^{-i\frac{Jt}{\hbar}(\omega_p^1-\omega_p^3)}|\mathcal{T}_{11}^p|^2 + e^{-i\frac{Jt}{\hbar}(\omega_p^2-\omega_p^4)}|\mathcal{T}_{22}^p|^2 + e^{-i\frac{Jt}{\hbar}(\omega_p^1-\omega_p^4)}|\mathcal{T}_{12}^p|^2 + e^{-i\frac{Jt}{\hbar}(\omega_p^2-\omega_p^3)}|\mathcal{T}_{21}^p|^2 + e^{-i\frac{Jt}{\hbar}(\omega_k^1+\omega_k^2-\omega_k^3-\omega_k^4)}|\mathcal{T}_{11}^p\mathcal{T}_{22}^p - \mathcal{T}_{12}^p\mathcal{T}_{21}^p|^2}{1 + |\mathcal{T}_{11}^p|^2 + |\mathcal{T}_{22}^p|^2 + |\mathcal{T}_{12}^p|^2 + |\mathcal{T}_{21}^p|^2 + |\mathcal{T}_{11}^p\mathcal{T}_{22}^p - \mathcal{T}_{12}^p\mathcal{T}_{21}^p|^2}, \end{aligned} \tag{11}$$

with $\mathcal{T}^p_{ij} = (\mathcal{U}_p^{-1}\mathcal{V}_p)_{ij}$ (see the Appendix for details). Finally, we get the rate function associated with the quench from parameters g_0 to g_1, in the thermodynamic limit, as

$$\mathcal{F}(t) = -\int_0^{\frac{\pi}{2}} \frac{d\phi_p}{\pi} \log|G_p(t)|. \tag{12}$$

Now, the solutions of $|G_p(t)| = 0$ correspond to the critical times, denoted by t^*. In the case of the UXY model (i.e., $\lambda_2 = d = 0$), we get $\tau^p_{12} = \tau^p_{12} = 0$, making the τ^p matrix diagonal. Therefore, the expression for $G_p(t)$ simplifies to the form

$$G_p(t) = e^{-i\frac{Jt}{\hbar}(\omega^1_p+\omega^2_p)} \frac{\left(1+e^{-2i\frac{Jt}{\hbar}\omega^1_p}\left|\mathcal{T}^p_{11}\right|^2\right)\left(1+e^{-2i\frac{Jt}{\hbar}\omega^2_p}\left|\mathcal{T}^p_{22}\right|^2\right)}{\left(1+\left|\mathcal{T}^p_{11}\right|^2\right)\left(1+\left|\mathcal{T}^p_{22}\right|^2\right)}. \tag{13}$$

The solutions of $|G_p(t)| = 0$ lead to critical times $t^* = \frac{\hbar\pi}{J\omega^1_{p^*}}(n+\frac{1}{2})$, $n = 1, 2, 3, \ldots$ [10], which matches with the known results for the TFI model [8]. The equation for ω^2_p does not give any critical point. In the case of $\lambda_2 \neq 0$, such simplification does not happen, and therefore, for quenching onto any phases of the ATXY model (i.e., for $d\ (t > 0) = 0$), the solutions of $|G_p(t)| = 0$ are obtained numerically by a standard root-finding algorithm, which is naturally the case for the DATXY model. For details of the calculation of rate function, see the Appendix.

Note that the above treatment has to be generalized if the initial Hamiltonian $\hat{H}^{(0)}$ has degenerate ground states (see Refs. [8,9,15–17]). To keep things simple, we work with the fermionic version of the model, which is free from degeneracy in the AFM phase, and do not consider the CH phase as the initial one, since the above analysis has to be modified in that situation. However, the final parameters of the quench in the $(\lambda_1, \lambda_2, d)$ space can belong to any phase.

1. Nonuniformly spaced critical times

For the DATXY model, in general, the τ^p matrix has off-diagonal terms, which possibly lead to nonuniformly spaced critical times t^* on the time axis as depicted in Fig. 2. Note that this was not the case for the quantum XY model with a uniform magnetic field (UXY) or the TFI model [8].

2. Connection between DQPT and EQPT

For the TFI model in 1D, it was found that DQPTs are in one-to-one correspondence to the EQPTs [8,9], where the nonanalytic nature of the rate function was only observed for a quench across the EQPT line. However, later on, counterexamples in the UXY model were reported in Ref. [19], where such connections were absent. In the case of the DATXY model, the situation is much more involved and we summarize our observations below.

(i) For $d < \gamma$ and quenches from the AFM phase to one of the PM phases, or vice versa, the DQPT has one-to-one correspondence with the EQPT [see Fig. 3(d)]. However, if the anisotropy parameter γ is also quenched, such a connection no longer holds (see Ref. [19]).

(ii) As the PM phases of the DATXY model are connected by local transformations [74], one expects that quenching between these two phases does not result in a DQPT [see Fig. 3(e)]. On the contrary, our analysis shows the existence of DQPTs for some specific cases of such quenches [see Figs. 3(a)–3(c) and 3(f)].

(iii) For $d > 0$, a quench from a point in PM-II to another point in PM-II with different signs in λ_2 (involving a crossing of one or more gapless critical lines/regions) may result in a DQPT [Fig. 3(c)]. Note that this feature is special only to the PM-II phase and cannot be observed in any other phases for

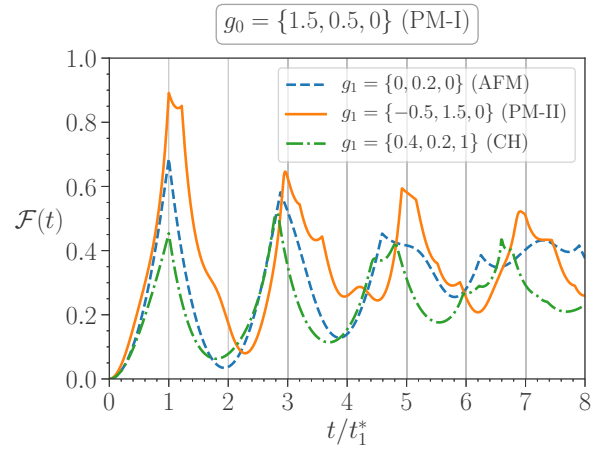

FIG. 2. Rate function $\mathcal{F}(t)$ vs t/t_1^*. The dynamics occurs due to quenches from the point $g_0 = \{1.5, 0, 0\}$, which lies in the PM-I phase, to three different points, namely, (i) $g_1 = \{0, 0.2, 0\}$ (AFM phase), (ii) $g_1 = \{-0.5, 1.5, 0\}$ (PM-II phase), and (iii) $g_1 = \{0.4, 0.2, 1\}$ (CH phase), in the parameter space of the DATXY model. All the quenches are across EQPT lines. Clearly, in all three cases, $\mathcal{F}(t)$ becomes nonanalytic for different critical times t^*. Here, we have normalized the time axis by the first critical time t_1^* in all three cases to highlight the fact that, in the DATXY model, the critical times are not uniformly spaced with each other. All quantities plotted are dimensionless.

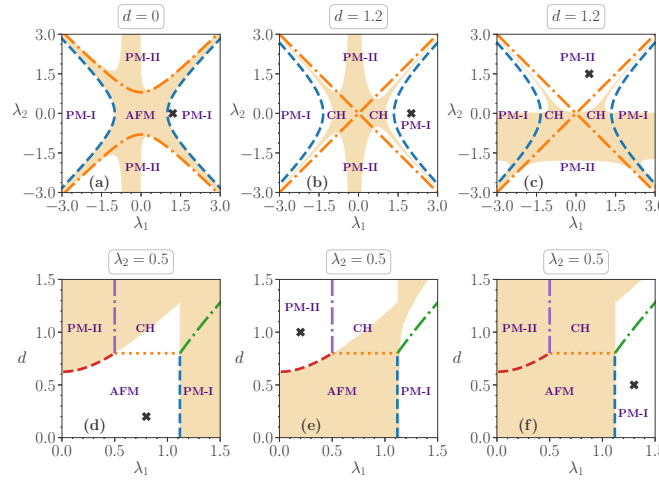

FIG. 3. DQPT regions in the parameter space of the DATXY model for the quenches from the points marked by ×. When a quantum quench is performed from a point, marked by the symbol ×, to any other point on the parameter space, only the shaded region shows nonanalyticity in the rate function given in Eq. (12). All the axes are dimensionless.

a fixed value of the anisotropy parameter γ. Such observation is akin to the quench of γ as seen in Ref. [19].

(iv) For $\lambda_2 = 0$ and fixed λ_1, quenching into the CH phase from the AFM phase by increasing d in the quantum quench does not result in a DQPT, as, in that case, the initial Hamiltonian, $\hat{H}[\lambda_1, 0, d(<\gamma)]$, and the final Hamiltonian, $\hat{H}[\lambda_1, 0, d(>\gamma)]$, commute with each other. However, with $\lambda_2 \neq 0$, a DQPT from the AFM to the CH phase is possible, provided the quenching is done sufficiently deep into the CH phase [Fig. 3(d)]. Similar features are observed for PM-I(II) $\rightarrow$ CH quenches [see Figs. 3(b), 3(c), 3(e), and 3(f)].

From the above observations, it is clear that, typically, there is no one-to-one connection between DQPT and EQPT phases in the DATXY model. However, all the observations reported here indicate that the *nonanalyticity of the rate function implies quench across at least a single critical line,* thereby providing us with a *necessary* condition for obtaining a DQPT. Next, we analyze the DQPT from an information-theoretic point of view and compare it with the Loschmidt-echo-based approach.

IV. ENTANGLEMENT AS A POTENTIAL DETECTOR OF DQPT

In the case of EQPTs, both bipartite entanglement and multipartite entanglement emerge as efficient detectors [1,77]. It was even shown that in some models, where the traditional detection methods fail, EQPTs could be detected by entanglement-based quantities [78,79]. Later, in other works [80–82], it was found that there exist models for which multipartite entanglement turns out to be better for identifying EQPTs compared to bipartite measures. In general, it has been realized that entanglement and other quantum correlation measures have the potential to detect EQPTs. The question then is: *Can entanglement be a "good" quantity to identify phase transitions that occur with the variation of time, after a sudden quench of parameters?*

We answer this question by analyzing the time evolution of bipartite entanglement and multipartite entanglement for the DATXY model after a sudden quench. Our analyses reveal that bipartite entanglement, contrary to its efficient EQPT detection capability for this model, turns out to be an inefficient detector of DQPT. First of all, the failure of bipartite entanglement as an identifier of DQPT for this model already once more underlines the difference between EQPT and DQPT from an information-theoretic perspective. Moreover, multipartite entanglement emerges as a good detector of DQPT.

A. Bipartite entanglement fails to detect DQPT

In this paper, we quantify bipartite entanglement via logarithmic negativity ($\mathcal{L}$). For an arbitrary two-party density matrix, ρ_{AB}, negativity ($\mathcal{N}$) and $\mathcal{L}$ are defined as

$$\mathcal{N}(\rho_{\rm AB}) = \tfrac{1}{2}\big(||\rho_{\rm AB}^{T_B}|| - 1\big) = \tfrac{1}{2}\big(||\rho_{\rm AB}^{T_A}|| - 1\big),$$
$$\mathcal{L}(\rho_{\rm AB}) = \log_2[2\mathcal{N}(\rho_{\rm AB}) + 1], \tag{14}$$

where $||A|| = {\rm tr}\sqrt{A^\dagger A}$ and $T_{A(B)}$ in the superscript of $\rho_{\rm AB}$ denotes partial transposition in the party $A(B)$. Note that, for $2 \otimes 2$ and $2 \otimes 3$ systems, negative partial transposition and hence nonzero $\mathcal{L}$ provides a necessary and sufficient condition for guaranteeing entanglement [83]. Thus, in our case, since all the two-site reduced density matrices have dimension $2 \otimes 2$, $\mathcal{L}$ is a faithful measure of entanglement.

Our analysis establishes that nearest-neighbor entanglement shows some qualitative changes when a quench is performed across a disorder to order transition, i.e., PM-I (II) $\rightarrow$ AFM/CH phase. Specifically, in these cases, the dynamics of $\mathcal{L}$ displays a distinctive *collapse and revival* feature. On the other hand, if the final parameters of the quench correspond to a disordered phase which is the same as the phase of the initial state, $\mathcal{L}$ does not show any collapse or revival and simply oscillates with decreasing amplitude, finally reaching a steady value.

However, note that the above features are only general trends and there exist several counterexamples to these patterns. Further investigation reveals that the dynamics of $\mathcal{L}$ shows a large overlap with the equilibrium phases and only has a weak connection with DQPT. Hence, we infer that bipartite entanglement is not an efficient detector of DQPT.

B. Effective definition of the generalized geometric measure (GGM)

Before presenting the results, let us define the entanglement measure that we use to study multipartite entanglement. For a set of states which are nongenuinely multipartite entangled, denoted by nG, the GGM of a state $|\psi\rangle$ is defined by

$$\mathcal{G}(|\psi\rangle) = 1 - \max|\langle\phi|\psi\rangle|^2, |\phi\rangle \in nG, \tag{15}$$

which, for an N-party pure state, reduces to

$$\mathcal{G}(|\psi\rangle) = 1 - \max\big\{\mu^{\rm max}_{i_1:{\rm rest}}, \mu^{\rm max}_{i_1 i_2:{\rm rest}}, \ldots, \mu^{\rm max}_{i_1 i_2 \ldots i_M:{\rm rest}}\big|$$
$$i_1, i_2, \ldots, i_M \in \{1, 2, \ldots \tilde{N}\}; i_k \neq i_l; k, l \in \{1, 2, \ldots M\}\big\}, \tag{16}$$

where $\tilde{N} = N/2$ or $(N-1)/2$ for even and odd lattice sizes, respectively, and $\mu^{\rm max}$ denotes the maximal eigenvalue of the reduced density matrices with rank equal to the number of i's present in the subscript of μ. Therefore, the evaluation of GGM, $\mathcal{G}(|\psi\rangle)$, boils down to the evaluation of the maximum of maximal eigenvalues for all reduced density matrices.

Although the evaluation of GGM has a clear prescription, its computation requires finding the maximum eigenvalues of $\binom{N}{1} + \binom{N}{2} + \cdots + \binom{N}{N/2} \sim 2^N$ number of matrices, which is definitely cumbersome for large N. However, from finite size analysis of the DATXY model with $N = 6$, 8, 10, and 12, we notice that for almost all times (except the initial response time $\sim \frac{2J}{\hbar}$) the maximal eigenvalue comes from either the single-site or the nearest-neighbor two-site reduced density matrices. Therefore, we can argue that even for systems with a large number of parties, the space consisting of the eigenvalues of single-site and nearest-neighbor two-site reduced density matrices remains the *effective* subspace for computing the GGM. Furthermore, we can exploit the translational invariance of the DATXY model to simplify the scanning space even for single-site and two-site reduced density matrices to just ρ_e, ρ_o, ρ_{eo}, and ρ_{oe}. Here $\rho_{e(o)}$ denotes the single-site (reduced) density matrix corresponding to even and odd sites, respectively, and $\rho_{eo(oe)}$ is the nearest-neighbor

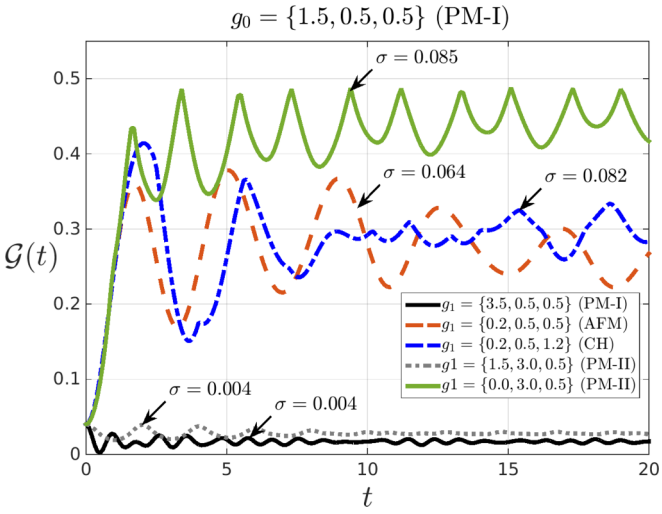

FIG. 4. Time variation of $\mathcal{G}$ after various quenches within and across equilibrium phases. We observe distinctly high amounts of fluctuations during the transient period of dynamics for specific regions (corresponding to DQPT, see Fig. 3) of disorder to order (PM-I to AFM and PM-I to CH) quenches and disorder to disorder (PM-I to PM-II) quenches, irrespective of the size of quench. Apart from these, other quenches show relatively lower amounts of fluctuations. Both the axes are dimensionless.

two-site density matrix between even-odd (odd-even) sites. Note that ρ_{eo} and ρ_{oe} have the same eigenvalues. Thus, in the thermodynamic limit ($N \to \infty$), the GGM can be effectively computed as

$$\mathcal{G}(|\psi\rangle) \approx 1 - \max\left\{\mu_{\rho_e}^{\max}, \mu_{\rho_o}^{\max}, \mu_{\rho_{eo}}^{\max}\right\}. \tag{17}$$

Note that even if in some situations the above argument does not remain valid, $\mathcal{G}(|\psi\rangle)$ still remains a measure of entanglement for multipartite states, providing an upper bound for the GGM. Furthermore, it also remains an local operations and classical communication (LOCC) monotone.

C. Advantages of multipartite entanglement as a detector of DQPT

We find that multipartite entanglement, $\mathcal{G}$, can capture DQPT when the quench corresponds to an underlying EQPT involving a disorder to order (PM-I/II $\to$ AFM/CH) transition or a disorder to disorder [PM-I(II) $\to$ PM-II(I)] transition. In particular, for a quench starting from the disordered phase, the dynamics of $\mathcal{G}$ displays a higher amount of oscillation for a quench that leads to a DQPT compared to those which do not start from such a phase (see Fig. 4).

For a quantitative treatment of the above observation, we estimate the amount of fluctuations in the time dynamics of $\mathcal{G}$ during the transient regime, by computing its time-averaged standard deviation, $\langle\sigma_{\mathcal{G}}(t)\rangle$, defined as

$$\langle\sigma_{\mathcal{G}}(t)\rangle = \frac{\hbar}{J\tau}\int_0^{\frac{J\tau}{\hbar}} \sigma_{\mathcal{G}}(t)dt, \tag{18}$$

where $\sigma^2_{\mathcal{G}}(t) = (\mathcal{G}^2(t) - \langle\mathcal{G}(t)\rangle)^2$, with $\mathcal{G}(t) = \mathcal{G}(|\psi(t)\rangle)$, and $|\psi(t)\rangle = e^{-i\hat{H}^{(1)}t/\hbar}|\Psi^0\rangle$. Note that for a reasonable average, τ should be taken to be large, but it should also be small

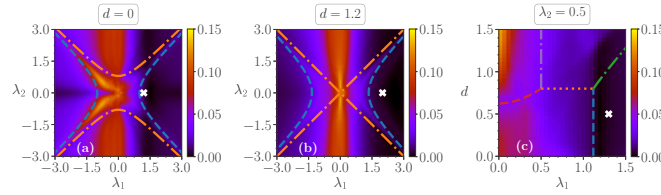

FIG. 5. Variation of the time-averaged standard deviation $\langle\sigma_{\mathcal{G}}(t)\rangle$, for quenches in the $(\lambda_1, \lambda_2, d)$ space with initial choices indicated by $\times$ as in Fig. 3. After the quench, we observe the emergence of a specific region in the (λ_1, λ_2) space in panel (a) and in the (λ_1, d) space in panel (b), which are distinctly characterized by high fluctuations, i.e., higher values of $\langle\sigma_{\mathcal{G}}(t)\rangle$. This region possess a high overlap with that depicted in Figs. 3(a), 3(b), and 3(f), which correspond to DQPTs, obtained by analyzing nonanalyticities in the rate function. This substantial overlap establishes multipartite entanglement as a good detector of DQPT. All the axes are dimensionless.

enough so that the system does not reach a steady state (i.e., $\tau_p < \tau \leqslant \tau_{\rm st}$, with $\tau_{\rm st}$ being the time at which the system enters a steady state and with τ_p being the approximate time period, in units of $J/\hbar$, of the oscillations), ensuring that the average is computed in the transient regime even as the effect of small variations in the oscillations are nullified. In our case, we choose $\tau = 20$ (with $\tau_{\rm st} \sim 50$). We analyze the variation of $\langle\sigma_{\mathcal{G}}(t)\rangle$ scanning the parameter space $(\lambda_1, \lambda_2, d)$ of the DATXY model. It is evident from Figs. 5(a)–5(c) [compare with Figs. 3(a), 3(b), and 3(f), respectively] that the value of $\langle\sigma_{\mathcal{G}}(t)\rangle$ is substantially larger for quenches that correspond to a DQPT and is confirmed by a large overlap of such regions with those detected by singularities in the rate function, thereby establishing multipartite entanglement, $\mathcal{G}$, as a *good* detector of DQPT.

Despite the advantages offered by multipartite entanglement, its DQPT detection capability is not ubiquitous. For example, if one starts from an ordered phase, the dynamics of $\mathcal{G}$ cannot detect DQPT. Therefore, the time variation of multipartite entanglement considered here can indicate the presence or absence of DQPTs only when the initial state parameters correspond to a disordered phase. A plausible explanation of this asymmetry can be provided by looking at the equilibrium GGM phase portrait which reveals that the ordered phases possess higher values of the GGM compared to the disordered phases (see Fig. 6). We find the GGM to be a "good" detector when the initial state possesses a low amount

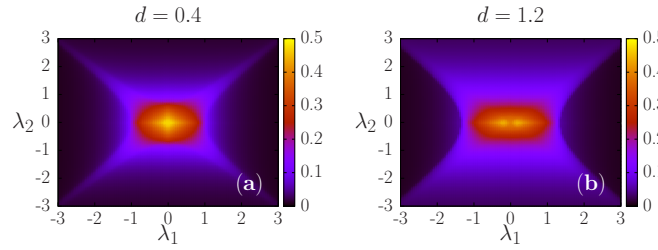

FIG. 6. The GGM phase portrait of the ground state of the DATXY model for (a) $d = 0.5$ and (b) $d = 1.2$, with respect to the uniform and alternate fields λ_1 and λ_2. The anisotropy parameter γ is fixed to 0.8. All axes are dimensionless.

of GGM, i.e., when the quench starts from a disordered phase. Note that there is no restriction on the GGM content of the ground state of the driving Hamiltonian. We want to stress here that we do not intend to replace the usual markers of many-body phases with the GGM, but rather to study the relationship of entanglement with DQPT and highlight that, for some quenches, the fluctuations in the GGM can actually indicate DQPT.

V. CONCLUSION

Dynamics of many-body systems reveal qualitative differences depending on the initial and quenched values of system parameters—known as dynamical quantum phase transition (DQPT). In this work, the analysis of DQPT is carried out for the DATXY (alternating field transverse XY model with Dzyaloshinskii-Moriya interaction) model after a sudden quench of system parameters. We *analytically* found that, in contradistinction to Ising systems, these systems possess nonuniformly spaced critical times (as indicated by the zeros of the Loschmidt echo) for the quenches which correspond to a DQPT. We also proposed a physical quantity based on multipartite entanglement as a good detector of DQPT.

The theory of DQPT, in essence, presents a quantitative formalism to understand the qualitative differences that occur during the dynamics of many-body systems after quenching of system parameters. Being intrinsically a feature of the transient regime, the analysis of DQPT is also of practical importance since one does not have to wait until equilibration to observe the relevant physics. Recent experimental realization of DQPT in various physical systems further reinforces the significance of such pragmatic studies.

ACKNOWLEDGMENTS

This research was supported in part by the INFOSYS Scholarship for Senior Students. T.C. was supported by Quantera QTFLAG Project No. 2017/25/Z/ST2/03029 of the National Science Centre (Poland). Computational work for this study was carried out at the cluster computing facility in the Harish-Chandra Research Institute [84]. We acknowledge the support from Interdisciplinary Cyber Physical Systems (ICPS) programme of the Department of Science and Technology (DST), India, Grant No. DST/ICPS/QuST/Theme-1/2019/23 (Project No. Q-121).

APPENDIX: CALCULATION OF THE RATE FUNCTION

The Loschmidt echo $L(t)$ is then described by the probability associated with this amplitude, i.e., $L(t) = |G(t)|^2$. The rate function associated with $L(t)$, which is analogous to the free energy (per lattice-site) in thermal phase transitions, can be defined as

$$\begin{aligned}\mathcal{F}(t) &= -\lim_{N\to\infty}\frac{1}{N}\log L(t)\\ &= -\lim_{N\to\infty}\frac{1}{N}\sum_{p=1}^{N/4}\log|G_p(t)|^2. \end{aligned}\tag{A1}$$

To deduce the analytical expressions of the Loschmidt amplitude and the rate function for a general quench from $g_0 \equiv \{\lambda_1(t=0), \lambda_2(t=0), d(t=0)\}$ to $g_1 \equiv \{\lambda_1(t>0), \lambda_2(t>0), d(t>0)\}$, we introduce the fermionic vector operator $\hat{A}_p = [\begin{smallmatrix}\hat{a}_p\\ \hat{b}_p\end{smallmatrix}]$, such that we can write $\hat{H}_p$ as $\hat{H}_p = J[\hat{A}_p^{\dagger T} \quad \hat{A}_{-p}^{T}]\tilde{H}_p[\begin{smallmatrix}\hat{A}_p\\ \hat{A}_{-p}^{\dagger}\end{smallmatrix}]$, with

$$\tilde{H}_p = \begin{bmatrix}(\cos\phi_p + d\sin\phi_p)\hat{\sigma}^x + \Lambda & -i\gamma\sin\phi_p\hat{\sigma}^x\\ i\gamma\sin\phi_p\hat{\sigma}^x & -(\cos\phi_p - d\sin\phi_p)\hat{\sigma}^x - \Lambda\end{bmatrix},\tag{A2}$$

where $\Lambda = \mathrm{Diag}\{\lambda_1 - \lambda_2, \lambda_1 + \lambda_2\}$. To diagonalize $\tilde{H}_p$ in Eq. (A2), we can perform the Bogoliubov transformation,

$$\begin{bmatrix}\hat{A}_p\\ \hat{A}_{-p}^{\dagger}\end{bmatrix} = M_p\begin{bmatrix}\hat{\Gamma}_p\\ \hat{\Gamma}_{-p}^{\dagger}\end{bmatrix} = \begin{bmatrix}U_p & -iV_p\\ -iV_p^* & U_p^*\end{bmatrix}\begin{bmatrix}\hat{\Gamma}_p\\ \hat{\Gamma}_{-p}^{\dagger}\end{bmatrix},\tag{A3}$$

with $\hat{\Gamma}_p = [\begin{smallmatrix}\hat{\eta}_p^a\\ \hat{\eta}_p^b\end{smallmatrix}]$, such that $\hat{H}_p$ is diagonal in the Bogoliubov basis $\{\hat{\eta}_p^{a\dagger}, \hat{\eta}_p^{b\dagger}, \hat{\eta}_{-p}^a, \hat{\eta}_{-p}^b\}$. U_p and V_p are Bogoliubov coefficients (matrices) that diagonalize $\hat{H}_p$ and are functions of $g \equiv \{\lambda_1, \lambda_2, d\}$. The fermionic algebra of $\hat{a}_p$, $\hat{b}_p$, $\hat{\eta}_p^a$, and $\hat{\eta}_p^b$ operators guarantee that the Bogoliubov matrix M_p is unitary in nature, i.e., $M_p^{-1} = M_p^{\dagger}$.

In order to calculate $\langle\Psi^0|\, e^{-iH^{(1)}t/\hbar}\,|\Psi^0\rangle$, we need to express $|\Psi^0\rangle$ in terms of Bogoliubov operators, $\{\hat{\Gamma}_p(g_1)\}$, that diagonalize $\hat{H}^{(1)}$, where $\hat{H}^{(i)} = \hat{H}(g_i)$, with g_0 representing the parameters of the Hamiltonian whose ground state is the initial state, while g_1 defines the parameters of the driving Hamiltonian. If the operators $\{\hat{\Gamma}_p(g_0)\}$ diagonalize the initial Hamiltonian $\hat{H}^{(0)}$, using Eq. (6), we arrive at the following relation:

$$\begin{aligned}\begin{bmatrix}\hat{\Gamma}_p(g_0)\\ \hat{\Gamma}_{-p}^{\dagger}(g_0)\end{bmatrix} &= M_p^{-1}(g_0)M_p(g_1)\begin{bmatrix}\hat{\Gamma}_p(g_1)\\ \hat{\Gamma}_{-p}^{\dagger}(g_1)\end{bmatrix},\\ &= \begin{bmatrix}\mathcal{U}_p(g_0,g_1) & -i\mathcal{V}_p(g_0,g_1)\\ -i\mathcal{V}_p^*(g_0,g_1) & \mathcal{U}_p^*(g_0,g_1)\end{bmatrix}\begin{bmatrix}\hat{\Gamma}_p(g_1)\\ \hat{\Gamma}_{-p}^{\dagger}(g_1)\end{bmatrix},\end{aligned}\tag{A4}$$

with

$$\begin{aligned}\mathcal{U}_p(g_0,g_1) &= U_p^{\dagger}(g_0)U_p(g_1) + V_p^T(g_0)V_p^*(g_1),\\ \mathcal{V}_p(g_0,g_1) &= U_p^{\dagger}(g_0)V_p(g_1) - V_p^T(g_0)U_p^*(g_1).\end{aligned}\tag{A5}$$

Calculation of $\mathcal{U}_p$ and $\mathcal{V}_p$ matrices entirely depends on the diagonalization of the 4×4 matrices $\tilde{H}_p(g_0)$ and $\tilde{H}_p(g_1)$ in Eq. (A2). Once the matrices $\mathcal{U}_p$ and $\mathcal{V}_p$ are obtained, we can write the initial state $|\Psi^0\rangle$ as a boundary state composed of

zero-momentum modes of $\hat{H}^{(1)}$, which is given by

$$|\Psi^0\rangle = \mathcal{N}^{-1} \exp\left[i \sum_{p=1}^{N/4} \hat{\Gamma}_p^{\dagger T} \left(\mathcal{U}_p^{-1}\mathcal{V}_p\right) \hat{\Gamma}_{-p}^{\dagger} \right] |0\rangle, \quad \text{(A6)}$$

where $|0\rangle$ is the ground state of $\hat{H}^{(1)}$, $\mathcal{N}$ is the normalization constant, and T denotes the transpose of the corresponding operators. If we now assume that the operators $\{\hat{\Gamma}_p(g_1)\}$ can diagonalize the Hamiltonian $\hat{H}^{(1)}$ in the way given by

$$\hat{H}_p^{(1)} = J\left[\hat{\Gamma}_p^{\dagger T}(g_1)\ \hat{\Gamma}_{-p}^{T}(g_1)\right] \begin{bmatrix} \hbar\omega_p^1 & 0 & 0 & 0 \\ 0 & \hbar\omega_p^2 & 0 & 0 \\ 0 & 0 & \hbar\omega_p^3 & 0 \\ 0 & 0 & 0 & \hbar\omega_p^4 \end{bmatrix} \begin{bmatrix} \hat{\Gamma}_p(g_1) \\ \hat{\Gamma}_{-p}^{\dagger}(g_1) \end{bmatrix}, \quad \text{(A7)}$$

with $\hbar\omega_p^k$ $(k = 1, 2, 3, 4)$ being the eigenvalues, then the Loschmidt amplitude, $G(t) = \langle\Psi^0| e^{-i\hat{H}^{(1)}t/\hbar} |\Psi^0\rangle$, reads as

$$G(t) = \frac{e^{i\frac{Jt}{\hbar}\sum_{p=1}^{N/4}(\omega_p^3+\omega_p^4)}}{\mathcal{N}^2} \langle 0| \exp\left[\sum_{p=1}^{N/4} \hat{\Gamma}_{-p}^{T}(g_1)\mathbf{M}_p\hat{\Gamma}_p(g_1) \right] \exp\left[\sum_{p=1}^{N/4} \hat{\Gamma}_p^{\dagger T}(g_1)\mathbf{N}_p\hat{\Gamma}_{-p}^{\dagger}(g_1) \right] |0\rangle, \quad \text{(A8)}$$

where

$$\mathbf{M}_p = \begin{bmatrix} -i\mathcal{T}_{11}^{p*} & -i\mathcal{T}_{21}^{p*} \\ -i\mathcal{T}_{12}^{p*} & -i\mathcal{T}_{22}^{p*} \end{bmatrix},$$
$$\mathbf{N}_p = \begin{bmatrix} ie^{-i\frac{Jt}{\hbar}(\omega_p^1-\omega_p^3)}\mathcal{T}_{11}^{p} & ie^{-i\frac{Jt}{\hbar}(\omega_p^1-\omega_p^4)}\mathcal{T}_{12}^{p} \\ ie^{-i\frac{Jt}{\hbar}(\omega_p^2-\omega_p^3)}\mathcal{T}_{21}^{p} & ie^{-i\frac{Jt}{\hbar}(\omega_p^2-\omega_p^4}\mathcal{T}_{22}^{p} \end{bmatrix}, \quad \text{(A9)}$$

with $\mathcal{T}_{ij}^p = (\mathcal{U}_p^{-1}\mathcal{V}_p)_{ij}$. Note that the ω_p^k's are eigenvalues of the matrix $\tilde{H}_p^{(1)}$, which is written as $\hat{H}_p^{(1)} = \hat{A}_p^{\dagger}\tilde{H}_p^{(1)}\hat{A}_p$, where $\hat{A}_p$ is the column vector $(\hat{a}_p, \hat{b}_p, \hat{a}_{-p}^{\dagger}, \hat{b}_{-p}^{\dagger})$, and the 4×4 matrix $\tilde{H}_p^{(1)}$ is given as

$$\tilde{H}_p^{(1)} = J \begin{bmatrix} (\lambda_1 - \lambda_2) & (\cos\phi_p + d\sin\phi_p) & 0 & -i\gamma\sin\phi_p \\ (\cos\phi_p + d\sin\phi_p) & (\lambda_1 + \lambda_2) & -i\gamma\sin\phi_p & 0 \\ 0 & i\gamma\sin\phi_p & -(\lambda_1 - \lambda_2) & -(\cos\phi_p - d\sin\phi_p) \\ i\gamma\sin\phi_p & 0 & -(\cos\phi_p - d\sin\phi_p) & -(\lambda_1 + \lambda_2) \end{bmatrix}, \quad \text{(A10)}$$

with $\phi_p \in [-\pi/2, \pi/2]$. Using Eqs. (A8) and (A9), and the prescription developed in Ref. [85], we get the Loschmidt amplitude per momentum mode for the DATXY model as

$$G_p(t) = e^{i\frac{Jt}{\hbar}(\omega_p^3+\omega_p^4)} \times \frac{1 + e^{-i\frac{Jt}{\hbar}(\omega_p^1-\omega_p^3)}|\mathcal{T}_{11}^p|^2 + e^{-i\frac{Jt}{\hbar}(\omega_p^2-\omega_p^4)}|\mathcal{T}_{22}^p|^2 + e^{-i\frac{Jt}{\hbar}(\omega_p^1-\omega_p^4)}|\mathcal{T}_{12}^p|^2 + e^{-i\frac{Jt}{\hbar}(\omega_p^2-\omega_p^3)}|\mathcal{T}_{21}^p|^2 + e^{-i\frac{Jt}{\hbar}(\omega_k^1+\omega_k^2-\omega_k^3-\omega_k^4)}|\mathcal{T}_{11}^p\mathcal{T}_{22}^p - \mathcal{T}_{12}^p\mathcal{T}_{21}^p|^2}{1 + |\mathcal{T}_{11}^p|^2 + |\mathcal{T}_{22}^p|^2 + |\mathcal{T}_{12}^p|^2 + |\mathcal{T}_{21}^p|^2 + |\mathcal{T}_{11}^p\mathcal{T}_{22}^p - \mathcal{T}_{12}^p\mathcal{T}_{21}^p|^2}, \quad \text{(A11)}$$

such that $G(t) = \prod_{p=1}^{N/4} G_p(t)$. Finally, we get the rate function associated with the quench from parameters g_0 to g_1, in the thermodynamic limit, as

$$\mathcal{F}(t) = -\int_0^{\frac{\pi}{2}} \frac{d\phi_p}{\pi} \log|G_p(t)|. \quad \text{(A12)}$$

Now, the solutions of $|G_p(t)| = 0$ correspond to the critical times, denoted by t^*. Clearly, nonanalyticity arises in $\mathcal{F}(t)$, if we can find real solutions (ϕ_p^*, t^*) of the transcendental equation

$$|G_p(t)| = 0, \quad \text{(A13)}$$

which describes a DQPT with the critical time t^*. As mentioned before, the matrix $\mathcal{T}$ and the eigenvalues $\{\omega_p^k; k = 1, 2, 3, 4\}$ can be computed easily by diagonalizing 4×4 matrices, $\tilde{H}_p(g_0)$ and $\tilde{H}_p(g_1)$, which, in turn, allows us to obtain $G_p(t)$ and thus the rate function $\mathcal{F}(t)$.

[1] B. K. Chakrabarti, A. Dutta, and P. Sen, *Quantum Ising Phases and Transitions in Transverse Ising Models* (Springer, Berlin, 1996).

[2] S. Sachdev, *Quantum Phase Transitions* (Cambridge University, Cambridge, England, 2009).

[3] S. Suzuki, J. Inoue, and B. K. Chakrabarti, *Quantum Ising Phases and Transitions in Transverse Ising Models* (Springer, Berlin, 2013).

[4] R. Horodecki, P. Horodecki, M. Horodecki, and K. Horodecki, Rev. Mod. Phys. **81**, 865 (2009).

[5] L. Amico, R. Fazio, A. Osterloh, and V. Vedral, Rev. Mod. Phys. **80**, 517 (2008).

[6] M. Lewenstein, A. Sanpera, V. Ahufinger, B. Damski, A. Sen(De), and U. Sen, Adv. Phys. **56**, 243 (2007).

[7] T. J. Osborne and M. A. Nielsen, Phys. Rev. A **66**, 032110 (2002).
[8] M. Heyl, A. Polkovnikov, and S. Kehrein, Phys. Rev. Lett. **110**, 135704 (2013).
[9] M. Heyl, Rep. Prog. Phys. **81**, 054001 (2018).
[10] A. Sen(De), U. Sen, and M. Lewenstein, Phys. Rev. A **72**, 052319 (2005).
[11] K. Sengupta, S. Powell, and S. Sachdev, Phys. Rev. A **69**, 053616 (2004).
[12] K. Sengupta, D. Sen, and S. Mondal, Phys. Rev. Lett. **100**, 077204 (2008).
[13] A. Sen, S. Nandy, and K. Sengupta, Phys. Rev. B **94**, 214301 (2016).
[14] A. Peres, *Quantum Theory: Concepts and Methods*, Fundamental Theories of Physics Vol. 57 (Springer, Berlin, 2006).
[15] M. Heyl, Phys. Rev. Lett. **113**, 205701 (2014).
[16] B. Žunkovič, M. Heyl, M. Knap, and A. Silva, Phys. Rev. Lett. **120**, 130601 (2018).
[17] S. A. Weidinger, M. Heyl, A. Silva, and M. Knap, Phys. Rev. B **96**, 134313 (2017).
[18] M. Heyl, Phys. Rev. Lett. **115**, 140602 (2015).
[19] S. Vajna and B. Dóra, Phys. Rev. B **89**, 161105(R) (2014).
[20] M. Heyl, Phys. Rev. B **95**, 060504(R) (2017).
[21] M. Heyl and J. C. Budich, Phys. Rev. B **96**, 180304(R) (2017).
[22] F. Andraschko and J. Sirker, Phys. Rev. B **89**, 125120 (2014).
[23] D. M. Kennes, D. Schuricht, and C. Karrasch, Phys. Rev. B **97**, 184302 (2018).
[24] P. Jurcevic, H. Shen, P. Hauke, C. Maier, T. Brydges, C. Hempel, B. P. Lanyon, M. Heyl, R. Blatt, and C. F. Roos, Phys. Rev. Lett. **119**, 080501 (2017).
[25] N. Fläschner, D. Vogel, M. Tarnowski, B. S. Rem, D.-S. Lühmann, M. Heyl, J. C. Budich, L. Mathey, K. Sengstock, and C. Weitenberg, Nat. Phys. **14**, 265 (2017).
[26] X.-Y. Guo, C. Yang, Y. Zeng, Y. Peng, H.-K. Li, H. Deng, Y.-R. Jin, S. Chen, D. Zheng, and H. Fan, Phys. Rev. Appl. **11**, 044080 (2019).
[27] E. Canovi, E. Ercolessi, P. Naldesi, L. Taddia, and D. Vodola, Phys. Rev. B **89**, 104303 (2014).
[28] S. Bose, Phys. Rev. Lett. **91**, 207901 (2003).
[29] T. J. Osborne and N. Linden, Phys. Rev. A **69**, 052315 (2004).
[30] M. Christandl, N. Datta, A. Ekert, and A. J. Landahl, Phys. Rev. Lett. **92**, 187902 (2004).
[31] R. Raussendorf and H. J. Briegel, Phys. Rev. Lett. **86**, 5188 (2001).
[32] M. H. Freedman, A. Kitaev, M. J. Larsen, and Z. Wang, Bull. Am. Math. Soc. **40**, 31 (2002).
[33] I. M. Georgescu, S. Ashhab, and F. Nori, Rev. Mod. Phys. **86**, 153 (2014).
[34] S. Roy, T. Chanda, T. Das, D. Sadhukhan, A. Sen(De), and U. Sen, Phys. Rev. B **99**, 064422 (2019).
[35] T. Moriya, Phys. Rev. **120**, 91 (1960).
[36] T. Moriya, Phys. Rev. Lett. **4**, 228 (1960).
[37] P. W. Anderson, Phys. Rev. **115**, 2 (1959).
[38] T. Siskens, H. Capel, and K. Gaemers, Physica A (Amsterdam, Neth.) **79**, 259 (1975).
[39] T. Siskens and H. Capel, Physica A (Amsterdam, Neth.) **79**, 296 (1975).
[40] J. Perk and H. Capel, Phys. Lett. A **58**, 115 (1976).
[41] J. Perk and H. Capel, Physica A (Amsterdam, Neth.) **92**, 163 (1978).
[42] O. Derzhko, T. Verkholyak, T. Krokhmalskii, and H. Büttner, Phys. Rev. B **73**, 214407 (2006).
[43] K. Maruyama, T. Iitaka, and F. Nori, Phys. Rev. A **75**, 012325 (2007).
[44] R. Jafari, M. Kargarian, A. Langari, and M. Siahatgar, Phys. Rev. B **78**, 214414 (2008).
[45] S. Chuan-Jia, C. Wei-Wen, L. Tang-Kun, H. Yan-Xia, and L. Hong, Chin. Phys. Lett. **25**, 817 (2008).
[46] R. Jafari and A. Langari, arXiv:0812.1862.
[47] M. Kargarian, R. Jafari, and A. Langari, Phys. Rev. A **79**, 042319 (2009).
[48] W. W. Cheng and J.-M. Liu, Phys. Rev. A **79**, 052320 (2009).
[49] X. S. Ma and A. M. Wang, Opt. Commun. **282**, 4627 (2009).
[50] J. H. H. Perk and H. Au-Yang, J. Stat. Phys. **135**, 599 (2009).
[51] C. Yi-Xin and Y. Zhi, Commun. Theor. Phys. **54**, 60 (2010).
[52] X. Hao, Phys. Rev. A **81**, 044301 (2010).
[53] Z. Kádár and Z. Zimborás, Phys. Rev. A **82**, 032334 (2010).
[54] B.-Q. Liu, B. Shao, J.-G. Li, J. Zou, and L.-A. Wu, Phys. Rev. A **83**, 052112 (2011).
[55] A. Das, S. Garnerone, and S. Haas, Phys. Rev. A **84**, 052317 (2011).
[56] B. Li, S. Y. Cho, H.-L. Wang, and B.-Q. Hu, J. Phys. A: Math. Theor. **44**, 392002 (2011).
[57] F.-W. Ma, S.-X. Liu, and X.-M. Kong, Phys. Rev. A **84**, 042302 (2011).
[58] Y. Yan, L. Tian, and L. Qin, Chin. Phys. B **21**, 100304 (2012).
[59] R. Jafari and A. Langari, Int. J. Quantum Inf. **09**, 1057 (2011).
[60] J. Vahedi and S. Mahdavifar, Eur. Phys. J. B **85**, 171 (2012).
[61] W. S. Cole, S. Zhang, A. Paramekanti, and N. Trivedi, Phys. Rev. Lett. **109**, 085302 (2012).
[62] H. T. Wang and S. Y. Cho, arXiv:1310.3169.
[63] E. Mehran, S. Mahdavifar, and R. Jafari, Phys. Rev. A **89**, 042306 (2014).
[64] M. Soltani, J. Vahedi, and S. Mahdavifar, Physica A (Amsterdam, Neth.) **416**, 321 (2014).
[65] G.-H. Liu, W.-L. You, W. Li, and G. Su, J. Phys.: Condens. Matter **27**, 165602 (2015).
[66] W. Chen and M. Sigrist, Phys. Rev. Lett. **114**, 157203 (2015).
[67] K. K. Sharma and S. N. Pandey, Quantum Inf. Process. **15**, 4995 (2016).
[68] A. Sen(De) and U. Sen, Phys. Rev. A **81**, 012308 (2010).
[69] A. Shimony, Ann. N. Y. Acad. Sci. **755**, 675 (1995).
[70] H. Barnum and N. Linden, J. Phys. A: Math. Gen. **34**, 6787 (2001).
[71] T.-C. Wei and P. M. Goldbart, Phys. Rev. A **68**, 042307 (2003).
[72] M. Blasone, F. Dell'Anno, S. De Siena, and F. Illuminati, Phys. Rev. A **77**, 062304 (2008).
[73] T. Chanda, T. Das, D. Sadhukhan, A. K. Pal, A. Sen(De), and U. Sen, Phys. Rev. A **94**, 042310 (2016).
[74] U. Divakaran, A. Dutta, and D. Sen, Phys. Rev. B **78**, 144301 (2008).
[75] S. Deng, L. Viola, and G. Ortiz, in *Recent Progress in Many-Body Theories*, edited by J. Boronat, G. E. Astrakharchik, and F. Mazzanti, Advances in Quantum Many-Body Theory Vol. 11 (World Scientific, Singapore, 2008).

[76] A. Dutta, G. Aeppli, B. K. Chakrabarti, U. Divakaran, T. F. Rosenbaum, and D. Sen, *Quantum Phase Transitions in Transverse Field Spin Models: From Statistical Physics to Quantum Information* (Cambridge University, Cambridge, England, 2015).

[77] L.-A. Wu, M. S. Sarandy, and D. A. Lidar, Phys. Rev. Lett. **93**, 250404 (2004).

[78] F. Verstraete, M. A. Martín-Delgado, and J. I. Cirac, Phys. Rev. Lett. **92**, 087201 (2004).

[79] I. Affleck, T. Kennedy, E. H. Lieb, and H. Tasaki, Commun. Math. Phys. **115**, 477 (1988).

[80] A. Biswas, R. Prabhu, A. Sen(De), and U. Sen, Phys. Rev. A **90**, 032301 (2014).

[81] R. W. Chhajlany, P. Tomczak, A. Wójcik, and J. Richter, Phys. Rev. A **75**, 032340 (2007).

[82] M. N. Bera, R. Prabhu, A. Sen(De), and U. Sen, arXiv:1209.1523.

[83] M. Horodecki, P. Horodecki, and R. Horodecki, Phys. Lett. A **223**, 1 (1996).

[84] http://www.hri.res.in/cluster.

[85] A. LeClair, G. Mussardo, H. Saleur, and S. Skorik, Nucl. Phys. B **453**, 581 (1995).